

PARTIAL FRACTIONAL FOURIER TRANSFORM (PFRFT)-OFDM FOR UNDERWATER ACOUSTIC COMMUNICATION

Yixin Chen, Carmine Clemente, John J. Soraghan and Stephan Weiss

Centre for Excellence in Signal and Image Processing (CeSIP), University of Strathclyde,
Royal College Building, 204 George Street, Glasgow, UK
E-mail: yixin.chen@strath.ac.uk, carmine.clemente@strath.ac.uk,
j.soraghan@strath.ac.uk, stephan.weiss@strath.ac.uk,

ABSTRACT

Communication over doubly selective channels (both time and frequency selective) suffers from significant intercarrier interference (ICI). This problem is severe in underwater acoustic communications. In this paper, a new Partial Fractional Fourier (PFRFT) based orthogonal frequency division multiplex (OFDM) scenario is presented for dealing with such challenges. A band minimum mean square error (BMMSE) weight combining equalizer based on Least Square MINRES (LSMR) iterative algorithm is used in the proposed communication system. Simulation results demonstrate significant BER performance improvements (up to 8dB) over traditional orthogonal based methods and those considering Partial FFT demodulation, and Discrete Fractional Fourier Transform (DFrFT) with only a moderate computational complexity increase.

Index Terms—Orthogonal frequency division multiplexing(OFDM),Partial Fractional Fourier Transform (PFRFT),Banded Minimum mean square error (BMMSE), Least Square MINRES (LSMR).

1. INTRODUCTION

Underwater acoustic communication (UWA) suffers from significant time delays reaching fractions of seconds as well as severe Doppler spread attributed to relative motion between transmitter and receiver. The problem is exacerbated due to the low speed of sound in water (1500m/s). Orthogonal Frequency Division Multiplexing (OFDM), is widely used in wireless communications that exhibits high dispersion due to its superior resistance to Inter-Symbol Interference (ISI) [1] and its low complexity. With an increase of subcarrier numbers, the bandwidth of each subcarrier will be smaller, therefore the system becomes more vulnerable to a loss in orthogonality caused by a high Doppler spread, leading to Inter-Carrier Interference (ICI) [2]. Recent research has focused on ICI suppression for enhanced performance with acceptable complexity. These mainly dealt with post-FFT processing methods, such as low complexity equalization. Banded

Minimum Mean Square Error (BMMSE) equalization was used in [3] on the band structure of channel frequency response. It was shown that the complexity increases linearly with the block length. However, the complexity of the BMMSE is lower than the conventional MMSE which is proportional to the cube of the number of subcarriers [3].

In [4]-[7] were introduced iterative detection and decoding techniques, such as the block turbo equalizer based on the exchange of soft extrinsic information between MMSE equalization, and maximum a posteriori probability (MAP) decoder. The banded equalization with iterative data detection has a superior robustness against errors of channel estimation, which usually occurs in the UWA scenario.

The Partial Fast Fourier Transform (PFFT) [2] [8] [9], decomposes a received signal into several segments using non-rectangular windows, followed by FFT demodulation and a weight compensation process on each segment. The working principle of the PFFT resides in the fact that the channel coherence time increases. This is achieved by increasing the bandwidth by splitting signal in time domain into several segments [9]. In [10] the conventional FFT demodulation in the OFDM was replaced by the Fractional Fourier Transform (FrFT), which transforms the signal into an intermediate domain between time and frequency. Doubly selective channel response will be concentrated into narrower band, allowing the ICI in adjacent subcarriers to concentrate around main diagonal of channel frequency matrix. The result presented in [10] showed a better performance with less complexity. FRFT could also be replaced by Fractional Cosine Transform (FRCT), as described in [11].

In this paper, a novel method called Partial Fractional Fourier Transform (PFRFT) is presented in conjunction with banded MMSE equalization enhanced communications over UWA channels. At the analysis stage, a doubly selective channel scenario is considered extracting simulated results showing the superior performance of the PFRFT approach compared with conventional PFFT and FrFT-OFDM ones. Moreover, the performance obtained

considering a low cost equalizer based on least squares (LSMR) approach [12] [13], which uses a tradeoff between performance and complexity are presented.

The remainder of paper is organized as follows. Section 2 presents the proposed PFrFT based algorithm that includes a DFrFT-OFDM block, the partial FFT demodulation and a low complexity ICI equalization based on LSMR iterative algorithm. A computational complexity analysis of the proposed system is also presented. In Section 3, simulation results and discussions are reported. Section 4 concludes the paper.

Notation: In this paper, transpose, conjugate and conjugate transpose are denoted as $[\cdot]^T$, $[\cdot]^*$ and $[\cdot]^H$ respectively. $\text{diag}\{\cdot\}$ denotes a diagonal matrix produced by a vector $[\cdot]_{i,j}$ extracts the i th row and j th column element from a matrix. Finally, $\langle \cdot \rangle_N$ is the modulo- N calculation.

2. SYSTEM MODEL

2.1. PFrFT based UWA Transceiver

The proposed PFrFT-OFDM system, as is shown in Figure1, is composed of several blocks. The uncoded N -point data vector \mathbf{d}_n is transformed into time domain using an inverse DFrFT of order α . The separate parallel data streams are then changed to a serial data after adding cyclic prefix. The serial received data stream corrupted by the UWA channel with additive white Gaussian noise \mathbf{v}_n is converted to a parallel data stream, which are processed by the partial FFT after removal of cyclic prefix. The LSMR iterative equalization is subsequently carried out on each partial block and converted to a bit stream using the DFrFT demodulation of order $(\alpha - 1)$. Each block of the system is described in details in the following section.

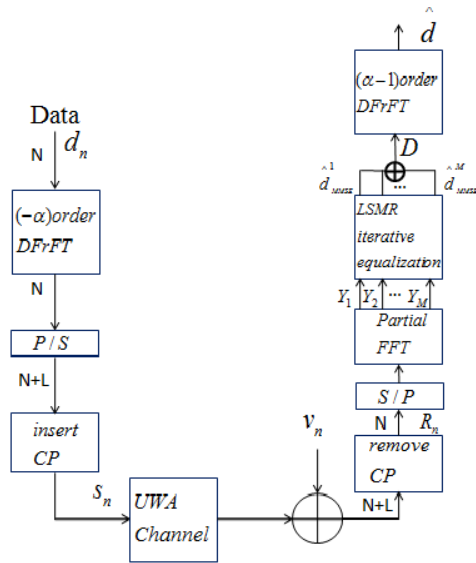


Figure1: Diagram of PFrFT-OFDM system with LSMR iterative equalization over doubly selective channel

2.2. Discrete Fractional Fourier Transform (DFrFT)

The Fractional Fourier transform (FrFT), first introduced by Namias [15], transforms a function of time into an intermediate domain between time and frequency, according to the rotation of time frequency distribution via angle θ or order α . In our previous work [10] [14], the Discrete FrFT (DFrFT) of order α presented in [10] was written in matrix vector multiplication as below:

$$\mathbf{y}_\alpha = \mathbf{F}_\alpha \mathbf{x} \quad (1)$$

Where:

$$\mathbf{y}_\alpha = [y_\alpha[0], y_\alpha[1] \dots y_\alpha[N-1]]^T, \\ \mathbf{x} = [x[0], x[1] \dots x[N-1]]^T,$$

and \mathbf{F}_α is the N point transformation matrix. Similarly, the inverse DFrFT is written as

$$\mathbf{x} = \mathbf{F}_\alpha^H \mathbf{y}_\alpha = \mathbf{F}_{-\alpha} \mathbf{y}_\alpha \quad (2)$$

It represents one of the main components of the proposed algorithm and is described in the next section.

2.3. Fractional Fourier transform OFDM system

In the DFrFT based OFDM scenario (DFrFT-OFDM), compared with conventional OFDM, the Discrete Fourier Transform (DFT) and inverse Discrete Fourier Transform (IDFT) blocks are replaced by the DFrFT and IDFrFT. Firstly, a binary matrix $\mathbf{J} \in \mathbb{Z}^{N \times N_a}$ is designed to allocate the data vector $\mathbf{d}_n \in \mathbb{C}^{N_a}$ to N subcarriers, written as

$$\mathbf{J} = \left[\mathbf{0}_{N_a \times (N-N_a)/2} \mathbf{I}_{N_a} \mathbf{0}_{N_a \times (N-N_a)/2} \right]^T \quad (3)$$

where $\mathbf{0}_{L \times M}$ is an $L \times M$ diagonal zero matrix, and \mathbf{I}_L is an $L \times L$ identity matrix.

The signal vector \mathbf{s}_n after the inverse DFrFT demodulation is corrupted by a doubly selective (DS) channel \mathbf{H}_t , producing received signal \mathbf{R}_n after discarding cyclic prefix

$$\mathbf{R}_n = \mathbf{H}_n \mathbf{s}_n + \mathbf{v}_n \\ = \mathbf{H}_n \mathbf{F}_{-\alpha} \mathbf{J} \mathbf{d}_n + \mathbf{F}_\alpha \mathbf{v}_n \quad (4)$$

where \mathbf{H}_n represents the time domain channel matrix characterized by

$$[\mathbf{H}_n]_{i,j} = \begin{cases} h[n-L+i, i-j] & i \geq j, \\ h[n-L+i, L+i-j-1] & i < j \end{cases} \quad (5)$$

The received signal after DFrFT demodulation can be then expressed as

$$\mathbf{R}_{df} = \mathbf{J}^H \mathbf{F}_\alpha \mathbf{H}_n \mathbf{s}_n + \mathbf{F}_\alpha \mathbf{v}_n \\ = \mathbf{J}^H \mathbf{F}_\alpha \mathbf{H}_n \mathbf{F}_{-\alpha} \mathbf{J} \mathbf{d}_n + \mathbf{F}_\alpha \mathbf{v}_n \\ = \mathbf{J}^H \mathbf{H}_{df} \mathbf{J} \mathbf{d}_n + \mathbf{F}_\alpha \mathbf{v}_n \quad (6)$$

If the channel is time invariant, \mathbf{H}_n is a convolutional matrix and the frequency channel matrix $\mathbf{H}_{df} = \mathbf{F}_{-\alpha} \mathbf{H}_n \mathbf{F}_\alpha$, is diagonal. However, when \mathbf{H}_{df} in a time varying channel, the channel matrix is not diagonal, and the energy spreads into adjacent subcarriers, contributing to ICI. The structure of \mathbf{H}_{df} becomes banded, with most significant elements around the main diagonal. Notice that, the complexity grows linearly with the length of the OFDM block, thus introducing the requirement of low-complexity equalization.

The binary matrix \mathbf{J} not only suppresses the adjacent channel interference, but also eliminates the coupling interference at the upper right and bottom left corner of \mathbf{H}_{df} .

2.4. Partial FFT demodulation

As shown in Figure 1, a partial FFT (PFFT) demodulation decomposes the received time domain signal into several segments using rectangular non-overlapping windows, followed by equalization on each segment. The principle of the PFFT is that the bandwidth increases with the number of segments, contributing to the coherence time of the channel to increase; it mitigates ICI caused by orthogonality loss.

The whole symbol duration of a received signal $\mathbf{R}_n = \{r_1, r_2, \dots, r_N\}^T$ is decomposed into M time segments using non-overlapping windows. The window can be written as follows

$$\mathbf{y}_m = \text{diag} \left\{ \underbrace{0, 0, \dots, 0}_{(m-1)Q}, \underbrace{1, 1, \dots, 1}_Q, \underbrace{0, 0, \dots, 0}_{N-mQ} \right\},$$

$$m = 1, 2, \dots, M \quad (7)$$

where $Q=N/M$ is the length of each segment

The m^{th} output after the PFFT demodulation is expressed as

$$\mathbf{Y}_m = \mathbf{J}^H \mathbf{F} \mathbf{Y}_m \mathbf{R}_n = \mathbf{H}_{fm} \mathbf{F}_{-\alpha+1} \mathbf{d} + \mathbf{J}^H \mathbf{F} \mathbf{Y}_m \mathbf{v}_n \quad (8)$$

In (8), the quantity $\mathbf{H}_{fm} = \mathbf{F} \mathbf{Y}_m \mathbf{H}_t \mathbf{F}^H$ is the coupling frequency response of channel at the m^{th} segment, and \mathbf{F} is the FFT operator. If the channel is time invariant, \mathbf{H}_{fm} will be a diagonal matrix and a single tap equalizer can be used as in conventional OFDM.

However, in a time varying channel, the energy between subcarriers will spread into neighbor subcarriers, leading to ICI, and thus alternative equalizers need to be considered.

2.5. Low complexity LSMR equalization

MMSE equalization [6] is used in order to suppress the ICI.

The masked channel matrix can be written as

$$\mathbf{B}_k = \begin{cases} [\mathbf{H}_{fm}]_{i, <i+u>N+1}, & -U \leq u \leq U \\ 0, & \text{otherwise} \end{cases} \quad (9)$$

where U is selected to be proportional to the Doppler bandwidth [3][7], leaving the non zero elements to be confined to U off-diagonals above and below the main diagonal of \mathbf{H}_{fm} . The weights of the MMSE equalizer based on the masked matrix, is given by

$$\mathbf{W}_{k, \text{MMSE}} = \mathbf{B}_k^H (\mathbf{B}_k \mathbf{B}_k^H + \frac{N_0}{M} \mathbf{I}_{2U+1})^{-1} \quad (10)$$

where N_0 denotes the noise variance calculated from signal to noise ratio (SNR)

The matrix inversion of a banded matrix in the MMSE equalizer leads to a significant increase in computational complexity over a single tap equalizer. A least squares MINRES (LSMR) [12] algorithm is applied to compute the matrix inversion iteratively, providing better performance with lower complexity.

The LSMR is an iterative algorithm for solving linear system $\mathbf{A}\mathbf{x} = \mathbf{b}$, such as least-squares (LS) problems $\min \|\mathbf{A}\mathbf{x} - \mathbf{b}\|_2$ and regularized least squares (RLS) $\min \left\| \begin{pmatrix} \mathbf{A} \\ \mathbf{1} \end{pmatrix} \mathbf{x} - \begin{pmatrix} \mathbf{b} \\ 0 \end{pmatrix} \right\|_2$ when \mathbf{A} is sparse or a fast linear operator.

The output from the MMSE may be expressed as

$$\hat{\mathbf{d}}_{\text{MMSE}} = \mathbf{W}_{k, \text{MMSE}} \mathbf{Y}_m$$

$$\mathbf{W}_{k, \text{MMSE}} \mathbf{Y}_m = \mathbf{B}_k^H (\mathbf{B}_k \mathbf{B}_k^H + \frac{N_0}{M} \mathbf{I}_{2U+1})^{-1} \mathbf{Y}_m \quad (11)$$

which can be changed to

$$(\mathbf{B}_k \mathbf{B}_k^H + \frac{N_0}{M} \mathbf{I}_{2U+1}) \hat{\mathbf{d}}_{\text{MMSE}} = \mathbf{B}_k^H \mathbf{Y}_m \quad (12)$$

which meets the requirement of regularized least squares problem $(\mathbf{A}^T \mathbf{A} + \mathbf{I})\mathbf{x} = \mathbf{A}^T \mathbf{b}$ and approximate solution with MMSE equalization is $\min \left\| \begin{pmatrix} \mathbf{A} \\ \mathbf{1} \end{pmatrix} \mathbf{x} - \begin{pmatrix} \mathbf{b} \\ 0 \end{pmatrix} \right\|_2$.

There are two parameters in the LSMR algorithm, the number of iterations and the signal to noise ratio (SNR) which relies on two significant factors: one is the noise level, and the other is the maximum Doppler and delay spread which determines the distribution of coefficients in channel matrix [12].

Further, the data estimation of each FFT segment $\hat{\mathbf{d}}_{\text{MMSE}}$ are added together,

$$\mathbf{D}_n = \sum_{m=1}^M \hat{\mathbf{d}}_{\text{MMSE}}[\mathbf{m}] \quad (13)$$

As is shown in Figure 1, the data detected in the frequency domain after equalization is converted back to the fractional domain using an α -order DFRFT domain by $(\alpha - 1)$ -order DFRFT, as follows

$$\hat{\mathbf{d}} = \mathbf{F}_{\alpha-1}[\mathbf{D}_n] \quad (14)$$

2.6. Complexity consideration

A comparative computational cost analysis per iteration between LSMR and BMMSE algorithms is given in Table I.

Table I

Computation for LSMR and BMMSE per iteration

Equalization algorithm	Computational optimization
LSMR	$O(N_a(U+1)I)$
BMMSE	$O(IU^3)$

It can be seen that the implementation of LSMR requires $O(N_a(Q+1)I)$ flops per iteration, where I is the number of segments implemented in the PFFT, which is less than the cost of the BMMSE which is $O(IU^3)$.

Table II

Total computation for PFrFT, DFrFT and PFFT system per iteration

methods	Computational complexity
PFrFT-LSMR	$O((I+1)N_a \log N_a) + O((U+1)I)$
DFrFT-LSMR	$O(N_a \log N_a) + O(U+1)$
PFFT-LSMR	$O(IN_a \log N_a) + O((U+1)I)$

Table II compares the total complexity of OFDM system based on PFrFT, DFrFT and PFFT. The complexity of the PFFT is $O(IN_a \log N_a)$, and that of DFrFT is $O(IN_a \log N_a)$. It can be seen that the superior performance of PFrFT over DFrFT comes at the cost of additional complexity. The complexity of PFrFT is similar to that of PFFT, due to the similarity between DFrFT and DFT. [1] [13]

3. SIMULATION RESULT AND DISCUSSION

The PFrFT-OFDM combined with iterative LSMR equalizer is simulated, and its performance compared to that from the conventional PFFT-OFDM and DFrFT-OFDM using banded equalization. The channel in this simulation is selected as doubly selective Rayleigh fading channel, which is fully known [1] [13].

3.1. Simulation set up

The number of symbols with QPSK modulation is $N=128$, of which $N_a = 96$ are active and the length of cyclic prefix is $L=8$. The normalized relative velocity between transmitter and receiver is $a = \frac{v}{c}=0.2742$, where c is the propagation speed. The normalized Doppler frequency is $isf_d T_d = 0.0014$. The UWA channel is modeled as Rayleigh fading channel with exponential multipath intensity profile of $[-7.2, -4.2, -6.2, -10.5, -12.2, -14.0]$ dB and time delay profile of $[0, 0.02, 0.05, 0.16, 0.23, 0.5]$ ms. The signal to noise ratio (SNR) ranges from 0 to 80dB. In addition, the low complexity equalizer is set at $U=3$ and the number Monte Carlo runs is 10000.

3.2. Simulation performance analysis

Figure 2 compares the BER performance of the partial Fractional Fourier Transform (PFrFT), Discrete Fourier Transform (DFrFT) and conventional partial Fourier Transform (PFFT) based OFDM scenarios with LSMR iterative equalization ($\alpha = 0.12$). The number of partial segments M is selected to be 8. It is seen that the performance of PFrFT-OFDM is superior to that of the PFFT-OFDM with a BER improvement of 5dB. One reason for positive results is that the non-zero band of the channel matrix in the fractional domain is significant lower than the conventional frequency domain, as illustrated in Figure 3.

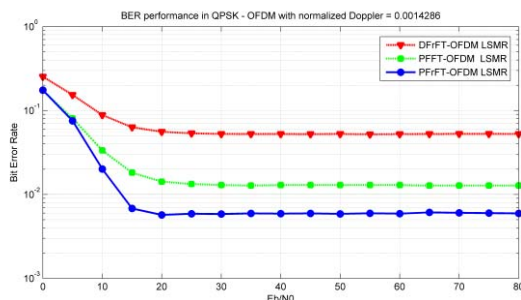


Figure2: BER of PFrFT-OFDM and PFFT-OFDM, and DFrFT-OFDM based on LSMR iterative equalization

The channel frequency matrices for both PFFT and PFrFT are shown in Figure 3(a) and 3(b) respectively. We assume that the channel frequency matrix \mathbf{H}_{df} is scalar into a grey level image, the value of which is in the range of $[0 \ 255]$. 0 means black and 255 means white. The bands, which are diagonal lines in both images with white color represent the energy of \mathbf{H}_{df} . The larger the energy, the closer the pixel value will be to 255. It can be ap-

preciated that the distribution of the band of PFFT distributes over more frequencies is than that of PFrFT, which means the energy of \mathbf{H}_{df} based on PFrFT concentrate closer to the diagonal, leading to less ICI and better BER performance.

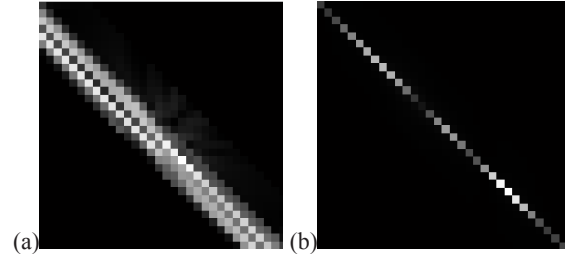


Figure3: channel frequency matrix (\mathbf{H}_{df}) of PFFT (a) and PFrFT (b)

Figure 2 shows that PFrFT-OFDM is superior to DFrFT-OFDM by approximately up to 8dB, attributed to the PFFT demodulation, which enables the outputs to contain minor mixing of contributions from different symbols. In addition, the bandwidth of the subcarriers increases while the received signal is decomposed into 8 segments in time domain. As detailed in Section 3, this performance result is achieved at the expense of an increase in complexity.

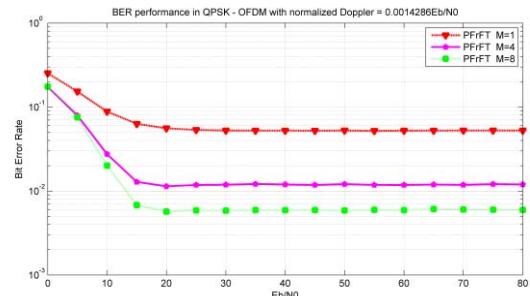


Figure4: BER of PFrFT-OFDM based on $M=1, 4$ and 8

Finally, Figure 4 compares the performance of PFrFT-OFDM based on different segments at $M=1, 4$ and 8 respectively. The results confirm that an improved BER is achievable using larger values of M . However it comes with an increase in computational cost.

4. CONCLUSION

In this paper, a novel concept of PFrFT-OFDM based on the hybrid use of the Discrete Fractional Fourier Transform (DFrFT), partial Fourier Transform (PFFT) demodulation and low complexity banded MMSE equalization has been proposed. The Least square MINRES (LSMR) equalizer was applied not only to improve the performance, but also to reduce the computational complexity. The ICI is significantly mitigated under doubly selective channel compared to the PFrFT-OFDM at moderate complexity providing an improvement in the overall Bit Error Rate.

ACKNOWLEDGEMENT

This work was supported by the Engineering and Physical Sciences Research Council (EPSRC) Grant number EP/K014307/1 and the MOD University Defence Research Collaboration in Signal Processing.

REFERENCE

- [1] S. Yerramalli, M. Stojanovic, and U. Mitra, "Partial FFT demodulation: A detection method for highly Doppler distorted OFDM systems," *IEEE Trans. Signal Process.*, vol. 60, no. 11, pp. 5906-5918, Nov. 2012.
- [2] M. Stojanovic and J. Preisig, "Underwater acoustic communication channels: Propagation models and statistical characterization," *IEEE Commun. Mag.*, vol. 47, no. 1, pp. 84-89, Jan. 2009.
- [3] P. Schniter, "Low-complexity equalization of OFDM in doubly selective channels," *IEEE Transactions on Signal Processing*, vol. 52, no. 4, pp. 1002-1011, April 2004.
- [4] B. Li, S. Zhou, M. Stojanovic, L. Freitag, and P. Willett, "Multicarrier Communication over underwater acoustic channels with nonuniform Doppler shifts," *IEEE J. Ocean. Eng.*, vol. 33, no. 2, pp. 198-209, Apr. 2008.
- [5] J. Huang, S. Zhou, J. Huang, C.R. Berger, and P. Willett, "Progressive inter-carrier interference equalization for OFDM transmission over time-varying underwater acoustic channels," *IEEE J. Sel. Topics in signal process.*, vol. 5, no. 8, pp. 1524-1536, 2011.
- [6] K. Fang, L. Rugini, and G. Leus, "Low-complexity block turbo equalization for OFDM systems in time-varying channels," *IEEE Trans. Signal Process.*, vol.56, no. 11, pp. 5555-5566, Nov. 2008.
- [7] L. Rugini, P. Banelli, and G. Leus, "Low-complexity banded equalizers for OFDM systems in Doppler spread channels," *EURASIP Journal on Applied Signal Processing*, vol. 2006, pp. 1-13, 2006.
- [8] Y. Li, X. Sha, F-C. Zheng and K. Wang, "Low Complexity Equalization of HCM Systems with DPFFT Demodulation over Doubly-Selective Channels," *IEEE Signal Processing Letters.*, vol. 21, no. 7, July 2014.
- [9] Y M. Aval, and M. Stojanovic, "Differentially Coherent Multichannel Detection of Acoustic OFDM Signals," *IEEE Journal of Oceanic Engineering*.
- [10] A. Solyman, S. Weiss and J.J. Soraghan, "Hybrid DFrFT and FFT based Multimode Transmission OFDM System." *presented at the ICEENG, 2012 Cairo, Egypt.*
- [11] A. Solyman, S. Weiss and J.J. Soraghan, "A Novel Orthogonal Chirp Division Multiplexing (OCDM) Multicarrier Transceiver Based on the Discrete Fractional Cosine Transform." *Presented at the MIC-WCMC, 2013 Valencia, Spain, 2013*
- [12] D.C.-L. Fong and M. A. Saunders, "LSMR: An iterative algorithm for sparse least-squares problems," *SIAM Journal on Scientific Computing*, March 2011.
- [13] A. Solyman, S. Weiss and J.J. Soraghan, "Low-Complexity LSMR Equalization of FrFT-Based Multicarrier Systems in Doubly Dispersive Channels," *presented at the ISSPIT 2011, Bilbao Spain, 2011.*
- [14] C. Candan, M. Kutay, and H. Ozaktas, "The discrete fractional Fourier transform," *IEEE Transactions on Signal Processing*, vol. 48, no.5, pp. 1329-1337, May 2000.
- [15] Namias, V., The Fractional Order Fourier Transform and its Application to Quantum Mechanics. *IMA Journal of Applied Mathematics*, 1980. 25(3): p. 241-265.